

# DQW HOM COUPLER DESIGN FOR THE HL-LHC\*

J. A. Mitchell<sup>†1</sup>, G. Burt, Lancaster University, Lancaster, UK  
 S. Verdú-Andrés, B. Xiao, BNL, Upton, NY 11973, USA  
 R. Calaga, CERN, Geneva, Switzerland  
<sup>1</sup>also at CERN, Geneva, Switzerland

## Abstract

HOMs in the DQW crab cavity can produce large heat loads and beam instabilities as a result of the high current HL-LHC beams. The DQW crab cavity has on-cavity, coaxial HOM couplers to damp the HOMs whilst providing a band-stop response to the fundamental mode. Manufacturing experience, LHC impedance thresholds and power considerations have given rise to a set of desirable coupler improvements. This paper will assess the performance of the current HOM coupler design, present operational improvements and propose an evolved design for HL-LHC.

## INTRODUCTION

The Double Quarter Wave (DQW) [1] for the HL-LHC upgrade [2] will firstly be tested in the Super Proton Synchrotron (SPS) at CERN. Two 400 MHz cavities, each with three Higher Order Mode (HOM) couplers have been manufactured and installed. Tests with beam will commence in the second quarter of 2018.

## SPS DQW HOM COUPLER

The current HOM coupler design, shown in Fig. 1, couples primarily to the cavity's magnetic field due to the 'hook-type' coupler. Following the hook, and also connected to the central shaft of the coupler, is a stub connected to a cylindrical 'jacket'. These provide the inductive and capacitive elements of the 400 MHz band-stop filter. The following section, up to the 50 Ω output line, acts as a high-pass filter which provides a power flux to an external load in case of HOM excitation by the beam.

The HOM couplers are made from niobium and internally cooled with 2 K liquid helium to reduce the chance of overheating which could lead to a field quench. They are de-mountable and as such require a flange and gasket. The location of the jacket is close to the hook to move it away from the flange location, minimising heating effects on the annealed copper gasket.

The cavity impedance reduction with the HOM couplers installed is used to evaluate and optimise their performance. The real part of the impedance value for each mode is calculated by multiplying the  $r/Q$  value [3] by the external quality-factor ( $Q_e \approx Q_l$  for superconducting cavities). To account for the effect of the mode's bandwidth on the impedance. The resonator model [4] is applied to each mode to produce the longitudinal impedance spectra shown in Fig. 2.

\* This work is supported by the HL-LHC project and Lancaster University.  
<sup>†</sup> j.a.mitchell@lancaster.ac.uk

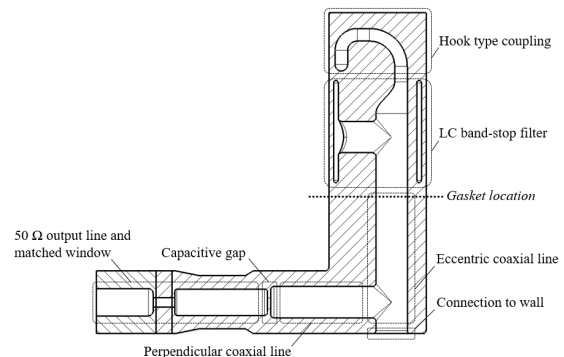


Figure 1: Two dimensional cross-section of SPS DQW HOM coupler's vacuum geometry.

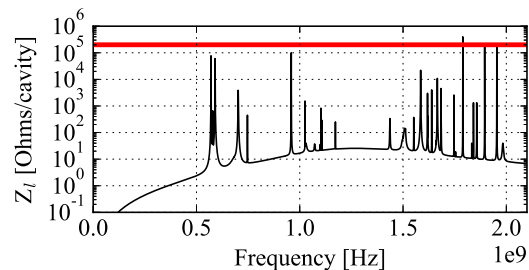


Figure 2: Longitudinal impedance spectra for the DQW dressed with the SPS couplers. The red line represents the design threshold.

The transverse impedance was calculated in the vertical and horizontal planes. The Panofsky-Wenzel theorem [5] was used to find the transverse voltage from the longitudinal voltage and the  $r/Q$  for the dipole component of each mode was used to form the transverse impedance spectra is shown in Fig. 3.

Specifications set out in [6] impose longitudinal and transverse impedance limitations of 200 kΩ/cavity and 1 MΩ/m/cavity respectively. This damping requirement has not been met by the SPS DQW HOM couplers and hence this was one of the main motivations for a re-design. This is in-part due to the limited space inside the cryomodule for the SPS DQW crab cavities. Due to the comparably small current of the SPS beam to that of the HL-LHC beam, ~100 mA to ~1.1 A, this impedance spectra was accepted for the test to verify HOM coupler performance with respect to simulations.

Convoluting the longitudinal impedance spectra and HL-LHC beam spectra [7], the power produced by the simulated

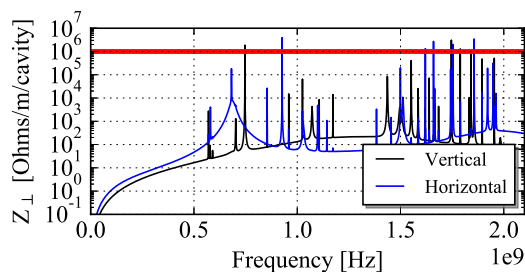


Figure 3: Transverse impedance spectra for the DQW dressed with the SPS couplers. The red line represents the design threshold.

DQW crab cavity and HOM couplers can be calculated. Figure 4 shows the spectral power plot up to the cut-off frequency of the 84 mm cylindrical beam pipes (2.01 GHz).

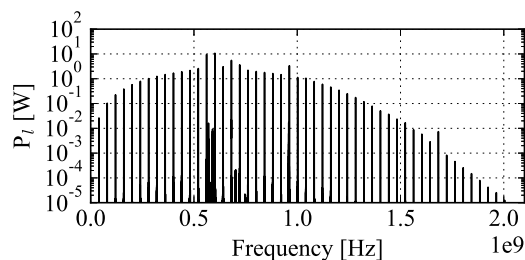


Figure 4: HOM power spectra for the DQW dressed with the SPS couplers.

The summation of the power is 83.6 W. This value is well within the threshold of the 1 kW specification for HL-LHC. However, this is representative of a DQW cavity where no mode frequency shift is observed. In reality, due to manufacturing errors, the measured value of mode frequency shift was  $\Delta f/f = 2.44 \times 10^{-3} \pm 2.97 \times 10^{-3}$ . The error corresponds to one standard deviation.

Investigating the summed power as a function of mode frequency showed that if a  $\Delta f/f$  deviation of  $3.17 \times 10^{-3}$  is applied to the mode at  $\sim 959$  MHz, the HOM couplers would be subjected to a power value of  $\sim 11$  kW due to an interaction with the 24<sup>th</sup> beam harmonic of the HL-LHC beam [7]. This is not only within the measured mode frequency deviation, but the measured deviations for SPS cavities 1 and 2 were  $3.64 \times 10^{-3}$  and  $3.11 \times 10^{-3}$  respectively. The detrimental frequency shift is hence feasible.

## OPTIMISATION

In addition to the RF optimisation goals presented, lessons learnt from the manufacture of the coupler resulted in some geometric improvement criteria.

### Manufacturing Improvements

The main difficulty experienced was welding the stub to the jacket, Fig. 5, and thus a flat section was incorporated on the jacket.



Figure 5: Manufactured SPS HOM coupler, with stub-jacket weld highlighted.

In addition to the weld, two other areas of difficulty were presented. The first was that producing a circular cross section is difficult and more time consuming to machine. Secondly, it is not possible to extrude the outer can to make the 90° bend as the outer diameter of the output line is flush with the base of the coupler. This adds cost as the part needs to be machined from bulk niobium.

To overcome the manufacturing difficulties, three changes were made. A flat section on the capacitive jacket was incorporated for welding of the stub, the profile was made rectangular and the output line was lifted with respect to the base of the coupler. The HOM coupler with the geometric alterations for manufacture is shown in Fig. 6.

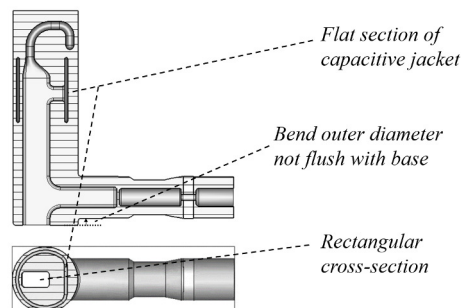


Figure 6: Vacuum geometry of the coupler with the manufacturing improvements.

### RF Optimisation

Initially the HOM coupler's equivalent circuit was used to analyse the transmission characteristics and effect of changing each element. Parametric studies were performed on both the equivalent circuit and the 3D model in CST MWS [8].

Weighting factors were defined for the effect of circuit elements (and hence coupler geometries) on the peaks of the coupler's transmission response. This allowed the amount of power flux at a given frequency to be altered to better damp the modes with impedance greater than the threshold as well as the 959 MHz mode. Geometric alterations and impedance simulations were iteratively performed to reduce the spectral impedance and HOM power. The HOM coupler's transmission characteristics, simulated on a cylin-

drical waveguide with one  $TE_{11}$  wave-guide port at a known but arbitrary distance from the coupling hook and a TEM wave-guide port on the output coaxial line, is displayed in Fig. 7.

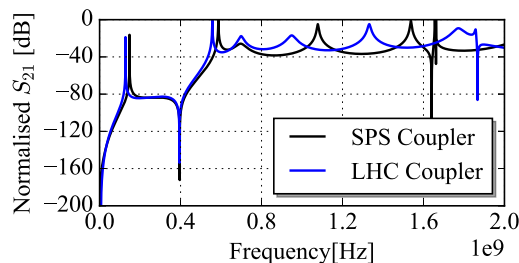


Figure 7:  $S_{21}$  for the SPS and LHC HOM couplers.

Using these HOM couplers on the cavity, the new impedance spectra were generated and can be seen in Fig.8.

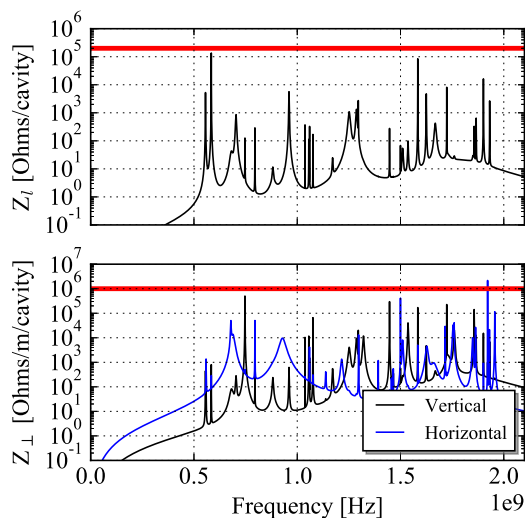


Figure 8: Longitudinal and transverse impedance spectra for the DQW crab cavity with the LHC HOM coupler.

All modes except one have an impedance within threshold. The mode at 1920 MHz has a vertical impedance of  $\sim 2 \text{ M}\Omega/\text{m}/\text{cavity}$ .

## LHC DESIGN - ANALYSIS WITH BEAM

If the power is again calculated as a function of frequency deviation of the mode at  $\sim 960 \text{ MHz}$ , the maximum for the new HOM coupler is reduced by a factor of 15 to  $\sim 720 \text{ W}$ . However, the new coupler geometry increases nominal frequency of the mode by 1.25 MHz, becoming closer to the frequency of the 24<sup>th</sup> beam harmonic.

To validate that the HOM power could not rise above the threshold, a stochastic normal distribution of  $\Delta f/f$  and  $\Delta Q_e/Q_e$  values were applied to each mode frequency, where the values for  $\sigma$  were taken from the deviation between the

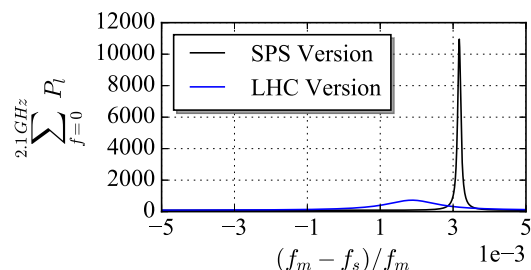


Figure 9: Summed power as a function of deviation of the  $\sim 960 \text{ MHz}$  mode frequency.

measured and simulated cases [9]. The average and maximum summed power values were calculated. This was repeated using the r/Q values data at several offsets, to additionally assess the effect of the beam moving off-axis. The resulting plots for both horizontal and vertical position are shown in Fig.10.

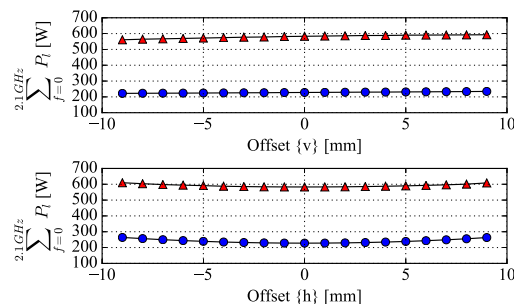


Figure 10: Summed power as a function of beam offset in the vertical and horizontal planes. The blue circles are the average values from the 1000 stochastic variations and the red triangles are the maximum.

## CONCLUSION

The impedance and power of the DQW crab cavities with the current HOM coupler geometries in HL-LHC conditions was assessed. A re-design of the HOM couplers was launched with the aim of easing the manufacture and meeting impedance and power thresholds.

Using equivalent circuit and 3D electromagnetic modelling. The impedance of all modes but one were reduced to below  $2 \text{ k}\Omega/\text{m}$  and  $1 \text{ M}\Omega/\text{m}/\text{cavity}$  for longitudinal and transverse modes respectively. The longitudinal power, even at the most detrimental mode frequencies, was reduced to below the 1 kW threshold.

## REFERENCES

- [1] R. Calaga *et al.*, "A DOUBLE QUARTER-WAVE DEFLECTING CAVITY FOR THE LHC", in *Proc. IPAC'13*, Shanghai, China, May. 2013, paper WEPWO047, pp. 2408–2410.
- [2] High-Luminosity Large Hadron Collider (HL-LHC), Preliminary Design Report, Edited by G. Apollinari, I. Béjar Alonso,

- Content from this work may be used under the terms of the CC BY 3.0 licence (© 2018). Any distribution of this work must maintain attribution to the author(s), title of the work, publisher, and DOI.
- O. Brüning, M. Lamont, L. Rossi, CERN-2015-005 (CERN, Geneva, 2015), DOI: <http://dx.doi.org/10.5170/CERN-2015-005>.
- [3] R. Wanzenberg, "Monopole, Dipole and Quadrupole Passbands of the TESLA 9-cell Cavity", in *TESLA 2001-33*, Sept. 2001.
- [4] I. Karpov, "HOM power in FCC-ee cavities", in *CERN-ACC-NOTE-2018-0005*, Jan. 2018.
- [5] W. Panofsky and W. Wenzel, in *Rev. Sci. Instrum* 27, 1956.
- [6] D. Amorim et al., "HL-LHC Impedance", CERN note for publication in 2018.
- [7] R. Tomás, Parameter update for the nominal HL-LHC: Standard, BCMS, and 8b+4e March. 2017
- [8] Computer Simulation Technology, *CST Microwave Studio 2015*, <https://www.cst.com/products/CSTMWS>.
- [9] J. Mitchell *et al.*, "Simulation and Measurements of Crab Cavity HOMs and HOM Couplers for HL-LHC", in *Proc. SRF'17*, Lanzhou, China, July. 2017, paper THPB059.